Inorganic Chemistry

Article

pubs.acs.org/IC

Understanding the "Tailoring Synthesis" of CdS Nanorods by O_2

Guoxin Zhang,† Peilei He,† Xiuju Ma,† Yun Kuang, Junfeng Liu,* and Xiaoming Sun*

State Key Laboratory of Chemical Resource Engineering, P.O. Box 98, Beijing University of Chemical Technology, Beijing 100029, People's Republic of China

Supporting Information

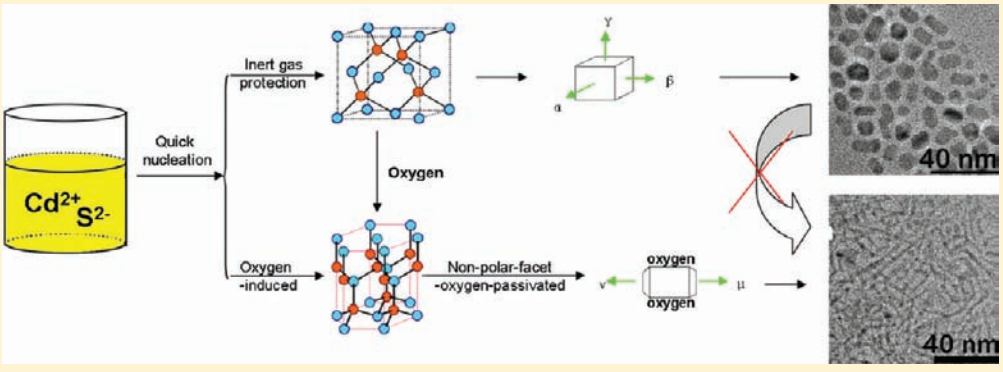

ABSTRACT: Parameters such as solution concentrations and composition of the ambient atmosphere are known to be important in phase and morphology control in the solvothermal synthesis of CdS semiconductor nanorods (NRs), but a clear understanding of the underlying mechanisms involved is lacking. In this work, a series of experiments were performed to demonstrate that the key factor affecting the phase and morphology of CdS NRs is the amount of O_2 in the space above the reaction solution in the sealed vessel relative to the amount of precursors in solution: O_2-depleted conditions resulted in more cubic phase CdS and thick polycrystalline NRs with an aspect ratio usually less than 3, which have small blue shifts in band-edge emission and little surface trap emission, while O_2-rich conditions resulted in more hexagonal-phase CdS and slim single-crystal NRs, which have significantly blue shifted band-edge emission and relatively strong surface trap emission. Thus, increasing the amount of solution in the vessel, changing the ambient atmosphere from air to N_2, and increasing the reagent concentration all lower the molar ratio of O_2 to reagents and lead to more cubic phase and thicker NRs. The results indicate that the composition of the "empty" section of the reaction vessel plays as important a role as the composition of the liquid in determining the phase and morphology, something that has been overlooked in earlier work. A mechanism to explain the effect of oxygen on the nucleation and growth stages has been proposed on the basis of those results and further supported by shaking experiments and ZnS NR synthesis manipulation. The CdS NRs synthesized under different conditions showed obvious differences in photocatalytic activity, which indicated that controlling the synthetic process can lead to materials with tailored photocatalytic activity.

INTRODUCTION

The last several decades have witnessed the development and applications of II–VI semiconductor nanocrystals. These nanocrystals show quantum confinement effects and unique dimension-dependent optical and electrical properties and are considered promising candidates for applications in many fields, such as solar cells,[1] biological labels,[2,3] light-emitting diodes,[4−6] and electronic devices.[7] Tailored synthesis (in terms of both morphology and phase) of semiconductor nanocrystals is a precondition for controlling their properties. Many methods have been employed to fulfill this goal, including template methods,[8,9] the vapor–liquid–solid (VLS) method,[10,11] cation exchange,[12] the use of colloidal micelles,[13] and solvothermal methods.[14−16] Of these, solvothermal and hydrothermal methods have been widely applied due to their low cost, mild working conditions, reasonable product quality (e.g., narrow particle size distribution and good crystallinity), and high reproducibility.

The controlled synthesis of CdS, one such semiconductor nanocrystal, has attracted particular attention. There are a plethora of papers reporting its controlled synthesis, which have confirmed that the phase and morphology can be tailored by many factors, including the precursor,[17] the solvent,[15,16] the use of capping reagents,[18,19] and even the presence of impurities.[20] A clear understanding of the reasons for the observed tailoring under solvothermal conditions, however, is still lacking.

Capping agents are most commonly used to control the synthetic process. For instance, Li et al. used ethylenediamine as a solvent to synthesize CdS NRs.[16] In their subsequent work, ultrathin CdS NRs were successfully synthesized with the

Received: May 26, 2011
Published: January 5, 2012

   dx.doi.org/10.1021/ic201119c | Inorg. Chem. 2012, 51, 1302–1308

assistance of polyethyleneimine.[21] Other alkyl amines such as hexadecylamine[22] and oleylamine[14,23] have also been used to control the anisotropic growth of CdS and resulted in twin-rod,[24] triangular,[13,23] tetrapod,[18,24,25] and hyperbranched[26] nanocrystals. In contrast, addition of organic acids leads to isotropic growth of CdS.[27,28] Also, some unique structures such as pencil-shaped CdS have been formed when more than one capping reagent was employed.[29,30]

It has only recently been found that O_2 can also tailor the synthesis of quantum dots. Papadimitrakopoulos et al. showed that oxygen can passivate certain crystal facets, leading to the anisotropic growth of CdSe.[31,32] In another report, however, it was found that the presence of O_2 during the synthesis only influenced the photoluminescence properties of the product.[33] In order to understand the role of oxygen in tailoring the phases and morphologies of CdS NRs, herein a series of experiments have been carried out to study the relationship between the synthetic conditions (e.g., the ambient atmosphere, extent of filling of the reaction vessel, precursor concentrations, and static or shaken reaction vessels) and the structures and properties of the resulting CdS NRs (e.g., phase, length, diameter, aspect ratio, defects, and photoluminescence properties). A formation mechanism was proposed on the basis of the above results. Furthermore, the photocatalytic degradation of rhodamine B (RhB) was used to probe the difference in properties for CdS NRs synthesized under different conditions.

EXPERIMENTAL SECTION

Chemicals. All reagents were purchased from Beijing Chemicals Co. Ltd. and used as received without further purification.

Synthesis of CdS NRS.[14] In a typical synthesis, 0.5 mmol of $Cd(CH_3COO)_2{\cdot}2H_2O$ was added to 12.5 mL of oleylamine at room temperature. The mixture was stirred for 30 min to form a clear solution. Then 0.6 mmol of thioacetamide was added and the mixture stirred for another 15 min. The solution was then transferred into a Teflon-lined autoclave (40 mL) and heated to 160 °C and aged at that temperature for 24 h. The final products were collected by centrifugation and washed with ethanol and cyclohexane. The NRs were dispersed in organic solvents, such as cyclohexane and chloroform, for characterization.

Synthesis of CdS NRs under Different Ambient Atmospheres. CdS NRs were prepared following the same procedure described above except that, after being transferred into the autoclave, the system was degassed by bubbling nitrogen, oxygen, or argon for 1 h through the solution.

Synthesis of CdS NRs with Different Filling Ratios. CdS NRs were prepared following the same procedure described previously, using different volumes of the mixture of $Cd(CH_3COO)_2{\cdot}2H_2O$, thioacetamide, and oleylamine, to give filling ratios from 15% to 90%.

Synthesis of CdS NRs with Different Precursor Concentrations. CdS NRs were prepared by following the same procedure described previously, except that the amount of $Cd(CH_3COO)_2{\cdot}2H_2O$ and thioacetamide were increased, while maintaining their ratio. Cd and C_2H_5NS amounts from 0.25 and 0.3 mmol to 2.0 and 2.4 mmol, respectively, in 12.5 mL of oleylamine were chosen.

Synthesis of CdS NRs with Shaking. CdS NRs were prepared following the same procedure described above, with a filling ratio of 15%, except that the autoclave was shaken at 100 rpm in an orbital shaker.

Synthesis of ZnS NRs under Different Atmospheres. ZnS NRs were prepared following the same procedure as for synthesis of CdS NRs under different atmospheres, except that the amount of thioacetamide was increased to 1 mmol with 0.5 mmol of $Zn(CH_3COO)_2{\cdot}2H_2O$.

Preparation of Photocatalysts. CdS NRs were synthesized with different filling ratios in air using the above method. Exchange of organic ligands on the surface of CdS NRs with metal chalcogenide complexes was carried out according to the method reported[34] (see the Supporting Information for experimental details).

Photocatalytic Reaction. The photocatalytic activities of CdS NRs were evaluated using the degradation of rhodamine B (RhB) under ultraviolet light irradiation by a 500 W Xe lamp. The same lamp with a 380 nm cutoff filter was used to determine the visible light photocatalytic activities. In a typical process, 0.02 g of as-prepared MCC-capped CdS NRs were added to 100 mL of RhB solution (4.4 mg/L), and the solution was stirred for 1 h in the dark to reach adsorption equilibrium. The solution was then exposed to ultraviolet or visible light irradiation, aliquots of the mixture were collected and centrifuged at given time intervals, and the RhB degradation concentration was measured by UV−vis spectroscopy.

Characterization. Fluorescence characterization was performed in transmission mode on a Hitachi F-4500 spectrophotometer over the range 800−400 nm. Measurements were typically performed on the fractions in a 1 cm path length quartz cuvette with excitation at 360 nm. The absorption spectra were measured using a Unico 2802PC UV−vis spectrophotometer at room temperature. A transmission electron microscope (Hitachi H-800, operated at 200 kV) was used to evaluate the size and shape of the NRs. Samples were directly dried on carbon film supported on copper grids for TEM characterization. X-ray diffraction (XRD) patterns of samples were collected on a Shimadzu XRD-6000 diffractometer with Cu Kα radiation (40 kV, 30 mA, λ = 1.5418 Å).

RESULTS AND DISCUSSION

The method employed for controlled synthesis of CdS NRs was based on that developed by Li's group,[14] using thioacetamide and cadmium acetate as reagents under different conditions. Our previous work showed that the length/diameter distribution of the nanorods formed was affected by the ambient atmosphere: those in O_2 contained nanorods with a larger aspect ratio, while those in N_2 contained fatter nanorods.[35] This inspired us to further explore oxygen's role in the synthesis of CdS NRs.

Tailoring Effect of O_2 on the Synthesis of CdS NRs. In order to systematically reveal the role of oxygen, a series of experiments were carried out to study the relationship between the structure and properties of the resulted CdS NRs and the synthesis conditions, such as the ambient atmosphere, filling ratio of the vessel, precursor concentrations, and so on.

The CdS NRs synthesized under various ambient atmospheres showed different powder X-ray diffraction (XRD) patterns (Figure 1). The majority of the reflection peaks of the cubic zinc blende (JCPDS No. 10-0454) and hexagonal wurtzite (JCPDS No. 41-1049) phases overlap with each other, except the (103) reflection peak of the hexagonal phase at 47.84°, which can be taken as a measure of phase purity: the absence of the (103) peak indicates a pure cubic phase, a similar intensity of (103) peak as compared to that of nearby (110) and (112) peaks characterizes a pure hexagonal phase, and a lower intensity of the (013) peak as compared to that of the (110) and (112) peaks is an indication of a mixture of hexagonal and cubic phases. As shown in Figure 1, the presence of a weak diffraction peak at 47.84° in the XRD pattern of the NRs synthesized in Ar and N_2 indicate that it crystallized mainly in the cubic phase together with a small amount of hexagonal phase. This is in accord with our previous observation that CdS NRs synthesized under a N_2 atmosphere were mixed phase.[36] In contrast, the diffraction peaks of NRs synthesized in O_2 and air fit exactly to the pattern for hexagonal CdS. The peak at 26.38°, which belongs to the (001) plane of CdS nanorod, is obviously sharper than others in the XRD

dx.doi.org/10.1021/ic201119c | Inorg. Chem. 2012, 51, 1302−1308

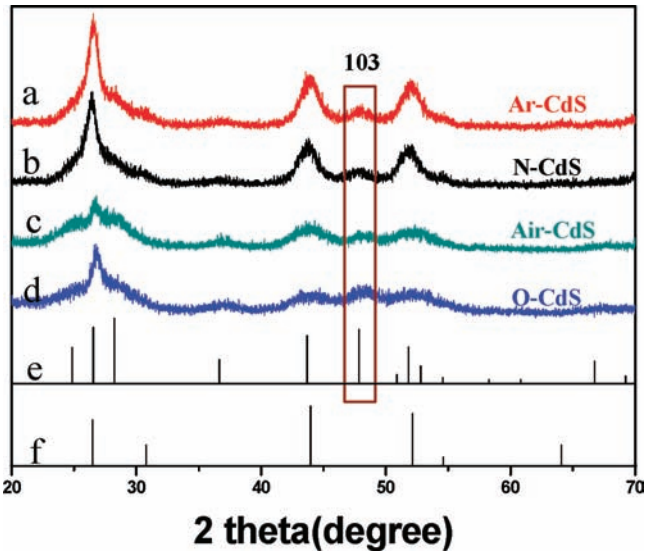

Figure 1. XRD patterns of CdS prepared in (a) Ar, (b) N_2, (c) air and (d) O_2. (e) Standard XRD data for the cubic phase from JCPDS file No. 41-1049. (f) Standard XRD data for the hexagonal phase from JCPDS file No. 10-0454.

pattern, indicating that these nanorods grow along the (001) direction, which was confirmed by our and other previous reports.[21,35]

In addition to the ambient atmosphere, the filling ratio (percentage of the volume of the autoclave occupied by the solution) and the precursor concentration are found to affect the final structures of CdS NRs. Figure 2A–D give TEM images of CdS NRs prepared with different filling ratios. Whent he filling ratio is increased from 15% to 90%, the NRs become thicker and shorter. XRD patterns (Figure 2E) show that the major phase changes from a hexagonal to a cubic phase as the filling ratio increases: the diffraction peaks of samples with filling ratios of 60% and 90% correspond to a mixture with a majority of the cubic phase, while the patterns of samples with filling ratios of 15% and 30% can be assigned to hexagonal CdS. These results showed that depletion of oxygen caused by high filling ratios favors the formation of thicker CdS NRs having the cubic phase, while greater amounts of oxygen direct the anisotropic growth to form thin CdS NRs with a hexagonal phase.

As is well known, CdS is a semiconductor with a band gap of ~2.4 eV, corresponding to band-edge emission at ~510 nm. Differences in NR diameters and surface states lead to different photoluminescence properties. As shown in Figure 2F, all the CdS NRs showed blue-shifted band-edge emission with the wavelength decreasing from 475 to 445 nm as their diameter decreased, due to the quantum size effect.[21,27] The intensity of surface trap emission photoluminescence at ~560 nm decreased markedly with increasing filling ratio, which is consistent with the effect induced by changing from a pure O_2 to a pure N_2 atmosphere (Figure S1, Supporting Information). This might be caused by the organic ligands used in the synthetic process, which makes it difficult to passivate all of the anions and cations on the surface of the NRs at the same time. Therefore, there are always S^{2-} anions or Cd^{2+} cations located in vacancies. Excitons may lead to recombination of these defects, resulting in nonradiative transition channels and leading to fluorescence at energies lower than the semiconductor band gap, as indicated by the surface trap emission in the region around 550 nm.[37,38] This trap-related electron–hole emission is particularly marked for the material synthesized in pure O_2, showing partial passivation by O_2.[39]

The concentrations of cadmium acetate and thioacetamide precursors were varied with a fixed filling ratio (30%) and O_2 concentration (air, 21% O_2). TEM images (Figure 3A–D) showed that higher precursor concentrations (and thus higher precursor to O_2 ratios) led to the formation of shorter and thicker CdS NRs with a lower aspect ratio. XRD data (Figure

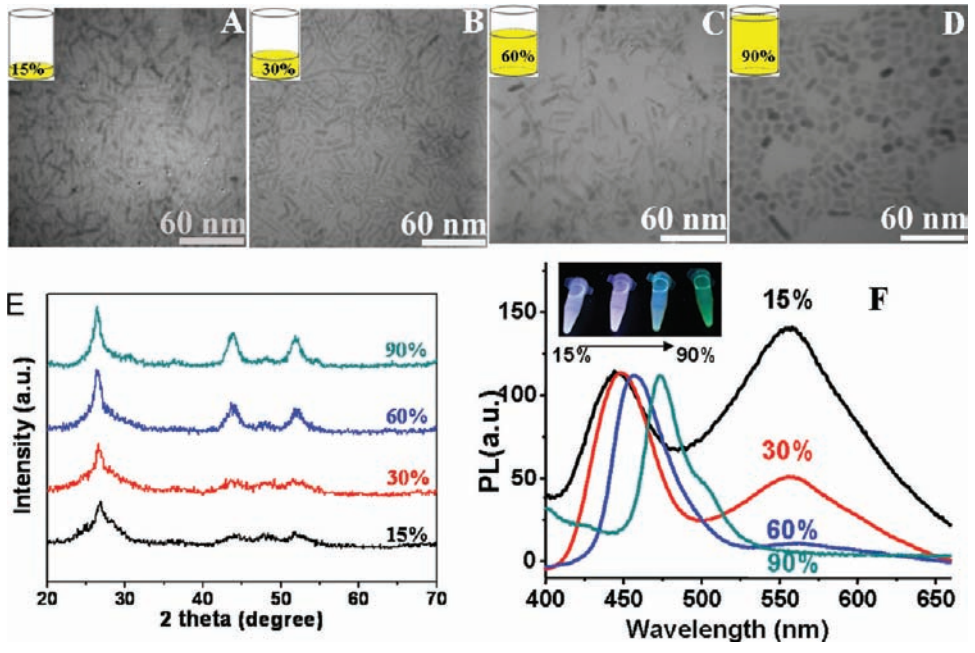

Figure 2. (A–D) TEM images of CdS NRs prepared with different filling ratios (15%, 30%, 60%, and 90%). (E) XRD patterns of CdS NRs prepared with different filling ratios. (F) Fluorescence spectra of CdS NRs prepared with different filling ratios. The inset shows solutions of A–D (from left to right) under UV irradiation at 365 nm.

dx.doi.org/10.1021/ic201119c | *Inorg. Chem.* 2012, 51, 1302–1308

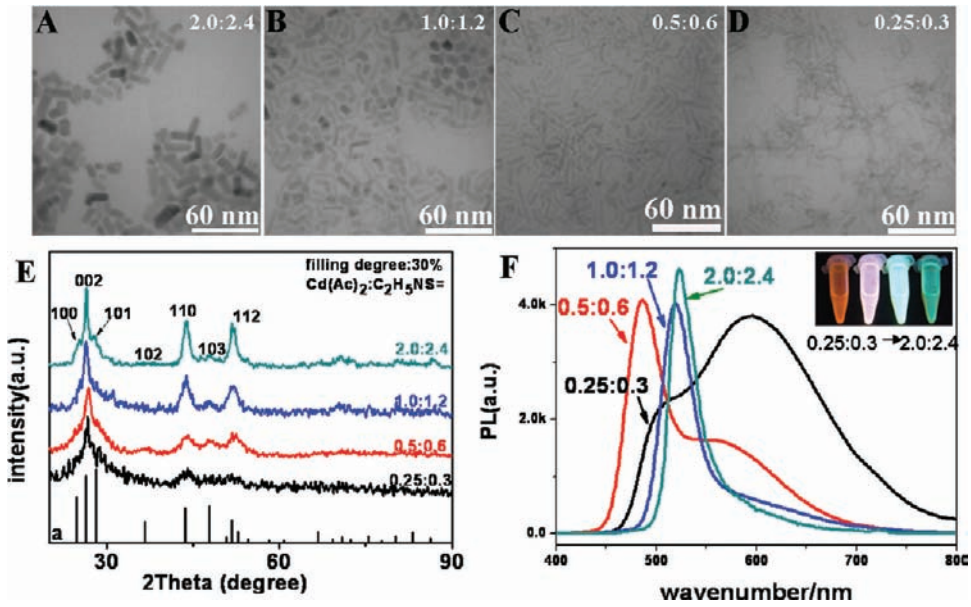

Figure 3. (A–D) TEM images of CdS NRs with different amounts of Cd and thioacetamide (C_2H_5NS) with the same reactor filling ratio of 30%. (E) XRD patterns of samples A–D from the top down and the standard pattern for the hexagonal phase of CdS JCPDS file No. 41-1049. (F) Photoluminescence spectra of samples A–D. The inset shows solutions of A–D (from left to right) under UV irradiation at 365 nm.

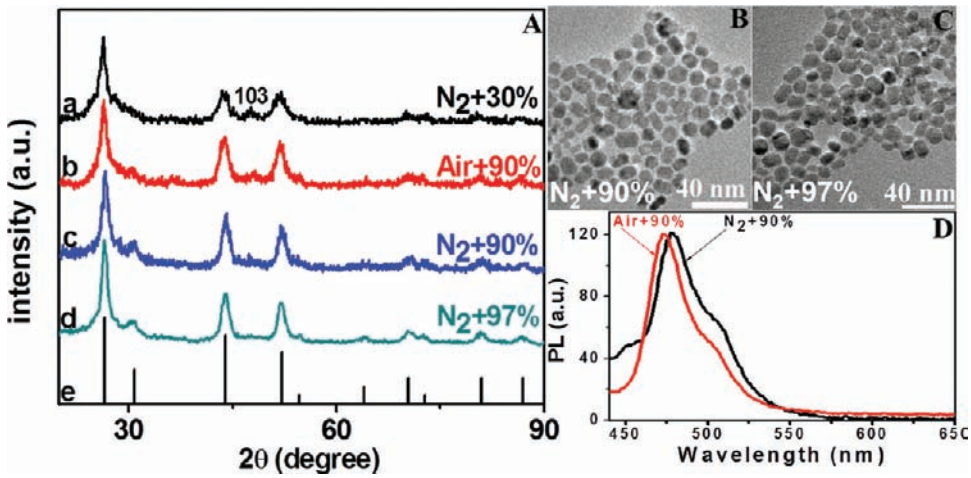

Figure 4. (A) XRD patterns of samples prepared with different ambient atmospheres and filling ratios: (a) N_2+30%; (b) Air+90%; (c) N_2+90%; (d) N_2+97%, with (e) standard XRD data for the cubic phase from JCPDS file No. 10-0454. (B) TEM image of CdS NRs (N_2+90%). (C) HRTEM image of CdS NRs (N_2+97%). (D) Fluorescence spectra of CdS NRs Air+90% and N_2+90%.

3E) revealed that higher precursor concentrations (i.e., low O_2:Cd and O_2:S ratios) led to more cubic phase being formed, as shown by the decreasing (103):(110) and (103):(112) peak intensity ratios. These results confirm that O_2-rich atmospheres lead to a stronger tendency to anisotropic growth and thinner NRs, and vice versa. NRs prepared with lower precursor concentrations showed larger blue shifts (Figure 3F), consistent with an O_2-rich environment. At the same time, the intensity of the surface trap emission at 550 nm increased as the precursor concentration decreased, which is also consistent with the increasing relative concentration of O_2.

The above experiments suggest that varying the ambient atmosphere, filling ratio, and precursor concentration all affect the synthesis through the same effect, by varying the relative concentration of O_2. To confirm this, and eliminate the possibility that other effects (such as the total pressure in the autoclave) are involved, two parameters were varied simultaneously. Two samples, one prepared with a filling ratio of 30% and purged with nitrogen (denoted 30%+N_2) and the other with a filling ratio of 90% but purged with air (denoted 90% +Air), were compared. Their XRD patterns (curves a and b in Figure 4A) showed no obvious differences and are consistent with the formation of a mixture of cubic and hexagonal phases, which suggested that the total gas pressure is not the key factor controlling the formation of CdS. By using a filling ratio of 90% but purging with N_2, an essentially pure cubic phase CdS was obtained (curve c). The slight red shift in the fluorescence on going from the sample 90%+Air to sample 90%+N_2 (Figure 4D) suggested that smaller NRs were obtained in the presence of air, which tailored the anisotropic growth of CdS NRs, leading to CdS NRs with smaller diameter. TEM images (Figure S3) of these two samples also gave a visual comparison, which clearly showed the sample 90%+Air was slightly smaller than the sample 90%+N_2. In order to obtain unambiguously

dx.doi.org/10.1021/ic201119c | Inorg. Chem. 2012, 51, 1302–1308

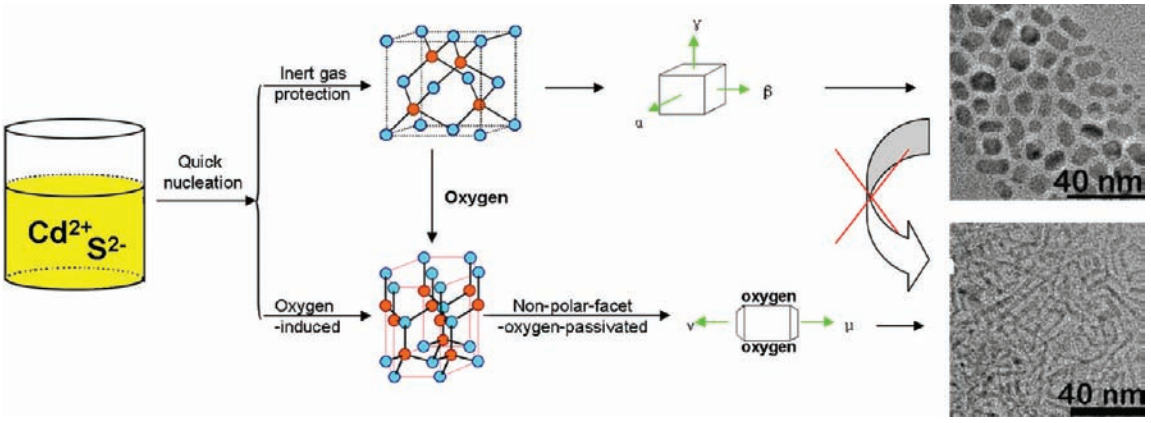

Figure 5. Schematic illustration of the effect of oxygen on the formation of CdS NRs.

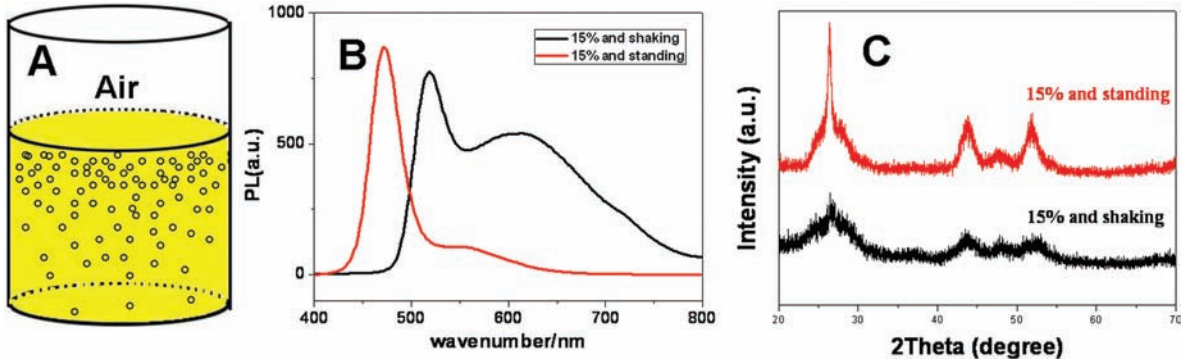

Figure 6. (A) Schematic illustration of the distribution of oxygen under static conditions. (B) Comparison of the fluorescence spectra of CdS NRs formed with a filling ratio of 15% under static conditions and with shaking. (C) XRD patterns of samples prepared with shaking and standing.

phase-pure cubic nanocrystals, a combination of purging with N_2 and increased filling ratio up to 97% was employed. The absence of any trace of the (103) reflection peak (curve d in Figure 4A) confirmed that the resulting CdS had a pure cubic phase. TEM (Figure 4B,C) showed that samples 90%+N_2 and 97%+N_2 consisted of mostly spherical nanocrystals, indicating isotropic growth. These data confirmed that small amounts of oxygen had a significant influence on both the phase and morphology, allowing the synthesis to be tailored.

Since we have shown that increasing the amount of oxygen dramatically tailors the growth of CdS and changes the crystal phase from cubic to hexagonal during synthesis, it is important to explore whether a similar effect could be observed when metastable cubic CdS meets oxygen. We synthesized pure cubic phase CdS NRs using a 97% filling ratio and purging with N and transferred them into autoclaves with 30% filling ratio that were purged with O_2 and then heated for 5 days. However, no phase change was found by XRD, shown by Figure S2A (in the Supporting Information). This indicates that a phase change cannot occur once the NR growth has terminated.

To our surprise, no shift in the surface trap related emission at ~560 nm was found, but a significant enhancement in the intrinsic band edge emission (Figure S2B, in the Supporting Information) was observed after this subsequent solvothermal treatment under O_2-rich conditions. This suggests that oxygen reacted with the NRs, resulting in strongly passivated sidewalls, which is consistent with Bard's observations[33] for CdSe nanocrystals.

Formation Mechanism and Supporting Experiments. The mechanism of formation of anisotropic CdS NRs (such as products with ultrathin, triangular, tetragonal, or hyperbranched structures) is of great significance. On the basis of the results discussed above, we proposed the following mechanism, as schematically shown in Figure 5. When Cd^{2+} and S^{2-} ions are released as the chemical reaction starts, CdS begins to nucleate and forms tiny nuclei. In the case of Ag nanoparticle synthesis[40,41] and tetrapod nanoparticle synthesis,[42] it has been shown that the formation of such nuclei is kinetically controlled, and they are polycrystalline in structure and mostly cubic in phase structure.[36,43] In the case of CdS, this polycrystallinity, the metastable nature of the cubic phase, and the extremely high surface area of these tiny nuclei make them extremely reactive to O_2. Thus, when sufficient O_2 is present, it reacts with the metastable nuclei and converts them to relatively thermally stable single-crystal hexagonal nuclei. O_2 passivates the sidewalls of the NRs and possibly forms Cd−O bonds; the absorbances cut off further growth perpendicular to the sidewall, thus leading to anisotropic growth along polar facets. Also, enough oxygen could react with S on the crystal surface to form SO_3^{2-}, similar to the known formation of SeO_3^{2-} in the case of CdSe,[32] and this should selectively absorb the amine from solution by an acid−base interaction and lead to anisotropic growth along polar facets. This anisotropic growth process leads to slim single-crystal CdS NRs with a hexagonal structure. Such passivation interferes with the formation of clean Cd−S crystal edges; more S or SO_3^{2-} vacancies will be obtained after this process, thus inducing more surface trap emission. However, in the absence of O_2, there is no such passivation and the nuclei retain the cubic structure. The resulting NRs inherit this cubic character and grow into

dx.doi.org/10.1021/ic201119c | Inorg. Chem. 2012, 51, 1302−1308

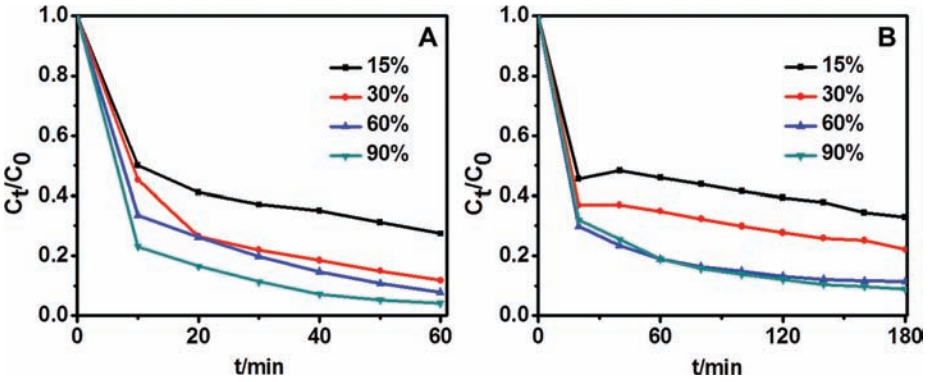

Figure 7. Variation of the degradation ratio of RhB by CdS NRs prepared with different filling ratios with irradiation time after (A) exposure to ultraviolet light irradiation and (B) exposure to visible light irradiation. C_0 and C_t represent the RhB concentrations before and after irradiation for time t.

thick CdS NRs, or even nearly spherical nanoparticles. Small amounts of O_2 will lead to the formation of a mixed phase. The resistance to phase conversion even after the 5 day reaction with sufficient oxygen tells us that the process is not reversible: oxygen can only tailor the "growing" CdS but not the "grown" NRs, although in the latter case the surface passivation does enhance the band edge emission.

If our hypothesis is correct, CdS NRs synthesized while mechanically shaking the mixture during the synthesis should be different from those synthesized under static conditions, where an O_2 concentration gradient should be created in the liquid medium due to migration/diffusion of oxygen, as shown in Figure 6A. Such a gradient should result in more O_2-passivated slim rods being formed near the surface where the O_2 concentration is high, but if the autoclave is shaken, this gradient will be eliminated, which should yield more monodisperse NRs. The results indicated that most of the products formed with shaking are rods with a certain aspect ratio. In contrast, a standing vessel will lead to form polydisperse rods and dots, shown by the TEM images in Figure S4 (Supporting Information). Indeed, for a 15% filling ratio we observed a strong surface trap emission for the CdS NRs formed by shaking during synthesis compared to that for those formed in a static reaction (Figure 6B), which should be relative to the more efficient use of oxygen in the autoclave by means of shaking. This was quite consistent with the XRD patterns (Figure 6C), which indicated more hexagonal-phase CdS formation.

In view of the similar crystal structures of CdS and ZnS, controlled synthesis of ZnS NRs was attempted under different ambient atmospheres (oxygen, air, and nitrogen) to confirm the mechanism of O_2 tailored synthesis. TEM images (Figures S3A–C, in the Supporting Information) showed that increasing the amount of oxygen led to longer and thinner ZnS NRs, which is consistent with what we observed for CdS and confirmed the proposed role of O_2 in the synthesis of II–VI nanocrystals. Figure S5D (in the Supporting Information) showed the variation in the length and length/diameter ratio of ZnS NRs under different ambient atmospheres, which demonstrates that more O_2 results in longer and slimmer ZnS NRs, further confirmed by XRD patterns (Figure S6, Supporting Information), which showed that the transfer from the cubic phase to the hexagonal phase corresponds to the reaction conditions varying from nitrogen protection to oxygen protection.

Photocatalytic Activity of CdS NRs. As shown above, the photoluminescence properties of CdS NRs varied for different morphologies. Therefore, the photocatalytic activity of the CdS NRs might also be different because they are both photo-irradiation-related procedures. In order to test the photo-degradation of dyes in aqueous solution, the hydrophobic CdS NRs must be transferred into an aqueous phase. The method reported by Talapin et al. was selected, in which oleylamine on the surface of CdS NRs was substituted by metal chalcogenide complexes (MCCs) in order to extract/transfer the CdS NRs into aqueous solution.[34]

The photocatalytic activities of the aqueous solutions of CdS NRs were evaluated using the degradation of rhodamine B (RhB) as a probe reaction. Figure S7 (in the Supporting Information) showed the UV–vis spectra of RhB solutions exposed to ultraviolet light in the presence of CdS NRs synthesized with different filling ratios (15% to 90% in air). Figure S8 (in the Supporting Information) showed the UV–vis spectra of the RhB solutions when exposed to visible light in the presence of the same set of NRs. The absorption peak at around 553 nm corresponded to RhB, and the absorption peak at 498 nm had been attributed to an intermediate in RhB degradation.[44] Figures S5 and S6 (in the Supporting Information) showed that CdS NRs synthesized with different filling ratios have distinctly different photocatalytic activities. Plots of C_t/C_0 vs t (Figure 7) showed that the activity of CdS NRs in the degradation of RhB is enhanced by increasing the filling ratio during the synthesis.

As shown in Figure 2, the band gap of CdS NRs decreases as the filling ratio during the synthesis is increased from 15% to 90% in air (Figure 2E). The photocatalytic results show that the narrower band gap is correlated with a higher photocatalytic activity for both UV and visible light irradiation. Our results suggest that researchers should pay more attention to controlling the amount of O_2 during synthesis in order to achieve CdS NRs with high photocatalytic activity.

■ CONCLUSION

It has been found that O_2 plays a dominant role in tailoring the phase and morphology of CdS NRs and the composition of the "empty" section of an autoclave should always be considered in the synthesis of NRs. The effects of varying the filling ratio, precursor concentrations, and ambient atmosphere on the properties of the product all highlight the role of O_2. A mechanism has proposed which gives a clear understanding of

dx.doi.org/10.1021/ic201119c | Inorg. Chem. 2012, 51, 1302–1308

how an O_2-rich environment results in a hexagonal phase, higher aspect ratio, and stronger surface-trap emission but limited photocatalytic activity. Similar results were obtained for ZnS NRs. This research provides a new way to understand and optimize the synthesis of II−VI semiconductor nanocrystals.

■ ASSOCIATED CONTENT

Supporting Information

Text and figures giving experimental details, photoluminescence spectra of CdS prepared in N_2, Ar, air, and O_2, XRD pattern and photoluminescence spectra of CdS NRs before or after transferring into autoclaves with 30% filling ratio and purged with O_2 and then heated for 5 days, TEM images of ZnS NRs formed under different ambient atmospheres and plots of the length and the aspect ratio for the different samples, XRD curves of ZnS NRs formed under different ambient atmospheres (N_2, N-ZnS; air, A-ZnS; O_2, O-ZnS), and UV−vis spectra of RhB solutions at different times on exposure to ultraviolet light or visible light. This material is available free of charge via the Internet at http://pubs.acs.org.

■ AUTHOR INFORMATION

Corresponding Author

*E-mail: sunxm@mail.buct.edu.cn (X.S.); ljf@mail.buct.edu.cn (J.L.).

Author Contributions

†These authors contributed equally to this work.

■ ACKNOWLEDGMENTS

This work was supported by the NSFC, the 973 Program (2011CBA00503, 2011CB932403), the Foundation for Authors of National Excellent Doctoral Dissertations of the People's Republic of China, the Program for New Century Excellent Talents in Universities, and the Beijing Natural Science Foundation.

■ REFERENCES

(1) Huynh, W. U.; Dittmer, J. J.; Alivisatos, A. P. *Science* **2002**, *295*, 2425−2427.
(2) Bruchez, M.; Moronne, M.; Gin, P.; Weiss, S.; Alivisatos, A. P. *Science* **1998**, *281*, 2013−2016.
(3) Chan, W. C. W.; Nie, S. M. *Science* **1998**, *281*, 2016−2018.
(4) Colvin, V. L.; Schlamp, M. C.; Alivisatos, A. P. *Nature* **1994**, *370*, 354−357.
(5) Tessler, N.; Medvedev, V.; Kazes, M.; Kan, S.; Banin, U. *Science* **2002**, *295*, 1506−1508.
(6) Coe, S.; Woo, W.-K.; Bawendi, M.; Bulovic, V. *Nature* **2002**, *420*, 800−803.
(7) Huang, Y.; Lieber, C. M. *Pure Appl. Chem.* **2004**, *76*, 2051−2068.
(8) Lv, R. T.; Cao, C. B.; Zhai, H. Z.; Wang, D. Z.; Liu, S. Y.; Zhu, H. S. *Solid State Commun.* **2004**, *130*, 241−245.
(9) Wang, Y.; Wu, Q. S.; Ding, Y. P. *J. Nanopart. Res.* **2004**, *6*, 253−257.
(10) Ge, J. P.; Li, Y. D. *Adv. Funct. Mater.* **2004**, *14*, 157−162.
(11) Wu, Y. Y.; Yang, P. D. *J. Am. Chem. Soc.* **2001**, *123*, 3165−3166.
(12) Son, D. H.; Hughes, S. M.; Yin, Y. D.; Paul Alivisatos, A. *Science* **2004**, *306*, 1009−1012.
(13) Pinna, N.; Weiss, K.; Urban, J.; Pileni, M. P. *Adv. Mater.* **2001**, *13*, 261−264.
(14) Li, P.; Wang, L. Y.; Wang, L.; Li, Y. D. *Chem. Eur. J.* **2008**, *14*, 5951−5956.
(15) Li, Y. D.; Wang, Z. Y.; Ding, Y. *Inorg. Chem.* **1999**, *38*, 4737−4740.
(16) Li, Y. D.; Liao, H. W.; Ding, Y.; Qian, Y. T.; Yang, L.; Zhou, G. E. *Chem. Mater.* **1998**, *10*, 2301−2303.
(17) Peng, Z. A.; Peng, X. G. *J. Am. Chem. Soc.* **2000**, *123*, 183−184.
(18) Jun, Y.-w.; Lee, S.-M.; Kang, N.-J.; Cheon, J. *J. Am. Chem. Soc.* **2001**, *123*, 5150−5151.
(19) Kovalenko, M. V.; Bodnarchuk, M. I.; Talapin, D. V. *J. Am. Chem. Soc.* **2010**, *132*, 15124−15126.
(20) Shen, Q. H.; Liu, Y.; Xu, J.; Meng, C. G.; Liu, X. Y. *Chem. Commun.* **2010**, *46*, 5701−5703.
(21) Zhuang, Z. B.; Lu, X. T.; Peng, Q.; Li, Y. D. *J. Am. Chem. Soc.* **2010**, *132*, 1819−1821.
(22) Li, Y. C.; Li, X. H.; Yang, C. H.; Li, Y. F. *J. Mater. Chem.* **2003**, *13*, 2641−2648.
(23) Chen, W.; Chen, K. B.; Peng, Q.; Li, Y. D. *Small* **2009**, *5*, 681−684.
(24) Chen, M.; Xie, Y.; Lu, J.; Xiong, Y. J.; Zhang, S. Y.; Qian, Y. T.; Liu, X. M. *J. Mater. Chem.* **2002**, *12*, 748−753.
(25) Manna, L.; Milliron, D. J.; Meisel, A.; Scher, E. C.; Alivisatos, A. P. *Nat. Mater.* **2003**, *2*, 382−385.
(26) Gao, F.; Lu, Q.; Xie, S.; Zhao, D. *Adv. Mater.* **2002**, *14*, 1537−1540.
(27) Yu, W. W.; Peng, X. G. *Angew. Chem., Int. Ed.* **2002**, *114*, 2474−2477.
(28) Cao, Y. C.; Wang, J. H. *J. Am. Chem. Soc.* **2004**, *126*, 14336−14337.
(29) Voitekhovich, S. V.; Talapin, D. V.; Klinke, C.; Kornowski, A.; Weller, H. *Chem. Mater.* **2008**, *20*, 4545−4547.
(30) Saruyama, M.; Kanehara, M.; Teranishi, T. *J. Am. Chem. Soc.* **2010**, *132*, 3280−3282.
(31) Li, R. F.; Luo, Z. T.; Papadimitrakopoulos, F. *J. Am. Chem. Soc.* **2006**, *128*, 6280−6281.
(32) Doll, J. D.; Pilania, G.; Ramprasad, R.; Papadimitrakopoulos, F. *Nano Lett.* **2010**, *10*, 680−685.
(33) Myung, N.; Bae, Y.; Bard, A. J. *Nano Lett.* **2003**, *3*, 747−749.
(34) Kovalenko, M. V.; Bodnarchuk, M. I.; Zaumseil, J.; Lee, J. S.; Talapin, D. V. *J. Am. Chem. Soc.* **2010**, *132*, 10085−10092.
(35) Sun, X. M.; Ma, X. J.; Bai, L.; Liu, J. F.; Chang, Z.; Evans, D.; Duan, X.; Wang, J.; Chiang, J. *Nano Res.* **2011**, *4*, 226−232.
(36) Ma, X. J.; Kuang, Y.; Bai, L.; Chang, Z.; Wang, F.; Sun, X. M.; Evans, D. G. *ACS Nano* **2011**, *5*, 3242−3249.
(37) Spanhel, L.; Haase, M.; Weller, H.; Henglein, A. *J. Am. Chem. Soc.* **1987**, *109*, 5649−5655.
(38) Kumar, A.; Janata, E.; Henglein, A. *J. Phys. Chem.* **1988**, *92*, 2587−2591.
(39) Myung, N.; Bae, Y.; Bard, A. J. *Nano Lett.* **2003**, *3*, 747−749.
(40) Wiley, B.; Sun, Y. G.; Xia, Y. *Acc. Chem. Res.* **2007**, *40*, 1067−1076.
(41) Xiong, Y.; Washio, I.; Chen, J.; Sadilek, M.; Xia, Y. *Angew. Chem., Int. Ed.* **2007**, *46*, 4917−4921.
(42) Chu, H. B.; Li, X. M.; Chen, G. D.; Zhou, W. W.; Zhang, Y.; Jin, Z.; Xu, J. J.; Li, Y. *Cryst. Growth. Des.* **2005**, *5*, 1801−1806.
(43) Yu, J. H.; Joo, J.; Park, H. M.; Baik, S. I.; Kim, Y. W.; Kim, S. C.; Hyeon, T. *J. Am. Chem. Soc.* **2005**, *127*, 5662−5670.
(44) Tadashi, W.; Takuo, T.; Kenichi, H. *J. Phys. Chem.* **1977**, *81*, 1845−1851.